Improved theoretical methods for studies of defects in insulators: Application to the F center in LiF

Mark R. Pederson and Barry M. Klein
Condensed Matter Physics Branch, Naval Research Laboratory, Washington, D.C. 20375-5000
(Received 15 October 1987)

An F center in the lithium fluoride (LiF) crystal is investigated with use of the muffin-tin Green's-function formalism and a linear combination of atomic orbitals (LCAO) cluster method. Both of these methods properly embed the defect into the host crystal. With the latter method, we are able to include the defect-induced charge relaxation on many shells of nearest-neighbor atoms. We have employed several variants of the density-functional approximation which allow a more accurate description of the ground-state single-electron properties. These methods include an empirical adjustment of the perfect-crystal band gap [the "LDA scissor operator" (where LDA denotes local-density approximation)] as well as the inclusion of electronic self-interaction corrections. Since the validity of the density-functional formalism is questionable for obtaining excited-state properties, we have introduced a single particle-hole excited-state theory, which is based on many-electron arguments, in order to gain insight about the behavior of the excited-state effective potentials. We demonstrate that, in contrast to LDA, for localized excitations the long-range behavior of the effective excited-state potential should exhibit a $-1/r$ tail in neutral systems. While the qualitative behavior of the LDA potential differs from the effective excited-state potential, the self-interaction-corrected LDA potential of the highest occupied defect level exhibits the correct qualitative behavior. By allowing the excited state electron to move in the latter potential, an accurate excitation energy for the a_{1g}-t_{1u} absorption in LiF is obtained. Further, in contrast to the density-functional results, the self-interaction-corrected version of the theory correctly places the t_{1u} state below the conduction-band edge.

I. INTRODUCTION

The F center in LiF and other alkali halides has received a great deal of experimental[1-4] and theoretical[5-13] attention for nearly two decades. Experimentally, it is now well known that when a negative fluorine ion is removed, it is replaced by an electron occupying a state of a_{1g} symmetry in the ground state, forming a so-called F (color) center. Further, there is a rather broad ultraviolet-absorption peak which exhibits a maximum at 5.10 eV,[1-3,14] and has a zero-point half-width of 0.60 eV (Ref. 14) corresponding to an excitation of the defect level from an a_{1g} (s-type) state to a t_{1u} (p-type) state. The F center in LiF has also been the subject of many theoretical investigations, as it is one of the simplest defects. The formalism used in previous theoretical calculations include both restricted[10-12] and unrestricted[13] Hartree-Fock (HF) and the Slater-exchange approximation.[8,9] The computational techniques which have been applied to this system include linear combination of atomic orbitals (LCAO) and scattered-wave methods with a varying number of surrounding atomic shells used in describing effects due to the defect. Even with this relatively large amount of work, there is no apparent theoretical consensus on the size of the a_{1g}-t_{1u} excitation energy, as estimates range from 3.0 to 5.5 eV. There are several possible reasons for this rather wide range of theoretical "excitation energies." First, the differing number of nearest-neighbor shells used in various calculations makes meaningful comparisons between the results, and with experiment, difficult. Secondly, it has been increasingly clear that calculations based on the local-density approximation (LDA) should not be expected to lead to occupied and unoccupied orbital energies (eigenvalues) that may be used to quantitatively predict excitation energies.[15-18] Also, the effects of defect-induced lattice relaxation need to be included to obtain the full picture of the excitation process.

In this paper we report on several different approaches for the study of defects in ionic solids and apply them to the F center in LiF. We have employed two complementary computational schemes for carrying out our calculations, the muffin-tin Green's-function (MTGF) formulation[19-23] and a LCAO-based embedded-cluster approach,[24-26] both of which properly embed the defect into the host crystal. We discuss the MTGF and LCAO cluster methods in Sec. II. In Sec. III we present our LDA results. As expected from other results on ionic insulators, these LDA results lead to a correct qualitative description of the occupied electronic energy levels, but do not provide quantitative information regarding the relative positions of the occupied bands, their widths, the perfect-crystal band gap, or the exact locations of the defect levels within the valence-conduction band gap. Since there is little formal justification for utilizing the LDA to extract such information, in Sec. IV we introduce a many-electron variational argument which leads to a simple single-particle picture for localized excitations. This

argument allows one to obtain certain qualitative information about the excited-state effective potentials such as their asymptotic limits. We formally demonstrate that the LDA potential does not exhibit the correct qualitative behavior for a proper description of electronic excited states, but that, for localized excitations, the self-interaction-corrected[25–32] (SIC) version of the LDA does indeed lead to a qualitatively correct excited-state single-particle Hamiltonian. In Sec. V we present the SIC results for the F-center electron which compare very favorably with experiment.

II. COMPUTATIONAL FRAMEWORK

In order to carry out our calculations, we have utilized the MTGF and LCAO cluster methods, which each have certain advantages, for embedding the defect into the host crystal. While the MTGF method is an elegant and computationally efficient approach for embedding the defect into the crystal, our current version includes charge relaxation on the first-nearest-neighbor shell only and is limited to systems in which the environment around each atom is nearly spherical. For systems such as LiF, the latter is not expected to be restrictive, but the former is worrisome. In contrast, the LCAO cluster method relies on more of a brute-force embedding method, but allows us to study charge relaxation on an arbitrary number of nearest neighbors as well as allowing studies on systems containing nonspherical atoms. Further, the relaxation of the core states is treated on the same level as that of the valence states (at present, our MTGF codes utilize the frozen-core approximation, but this can be remedied in a straightforward manner). While some of these differences may not be important for the F center in LiF, the greatest motivation for developing our LCAO cluster codes is that this method is quite amenable to applications of the self-interaction correction which we discuss in Sec. V.

A. The linear combination of atomic orbitals cluster method

For performing our LCAO cluster calculations, we have represented both the potentials and wave functions in terms of Gaussian-type functions. The first step in the calculation is to obtain the self-consistent perfect-crystal potential, and to do this we have utilized the BANDAID package, which has been developed by Erwin *et al.*[33] With an application of the variational principle, it can be shown that the self-consistent defect wave functions must satisfy

$$[H_0+\Delta V]\psi_i=\varepsilon_i\psi_i \ , \tag{1}$$

$$H_0=-\tfrac{1}{2}\nabla^2+V_{\rm ext}+\int dr'\frac{\rho_c(\mathbf{r}')}{|\mathbf{r}-\mathbf{r}'|}+V_{\rm xc}[\rho_c] \ , \tag{2}$$

$$\Delta V=\int d\mathbf{r}'\frac{\rho_d(\mathbf{r}')-\rho_c(\mathbf{r}')}{|\mathbf{r}-\mathbf{r}'|}+V_{\rm xc}[\rho_d]-V_{\rm xc}[\rho_c]+\frac{\Delta Z}{r} \ . \tag{3}$$

In the above equation, ΔZ is the difference between the nuclear charge of the defect atom (in this case a vacancy) and that of the removed atom, and ρ_d and ρ_c are, respectively, the charge densities due to the defect and perfect crystal. Unless otherwise stated, Hartree atomic units are used above and throughout this paper.[34] The external potential $V_{\rm ext}$ is due to the nuclear Coulomb attraction of each atom in the perfect crystal. It is computationally convenient to represent ΔV as an expansion in terms of Gaussian functions. For neutral defects, provided the relaxation of the density is localized, the difference potential is also localized. As such, an accurate representation of the difference potential for a given iteration may be obtained by fitting it to a linear combination of Gaussian-type functions of the form

$$\Delta V=\frac{\Delta Z}{r}e^{-\beta r^2}+\sum_{i,\lambda}V_{i\lambda}g(\gamma_i,\lambda) \ . \tag{4}$$

In the above expression, λ is the shell index, and the function $g(\gamma_i,\lambda)$ is a properly symmetrized[35] linear combination of Gaussian functions centered on each site (R_s^λ) of shell λ. Both the linear and nonlinear parameters have been optimized using standard least-squares techniques.

To solve Eq. (1), the wave functions, ψ_i, are expanded in terms of a linear combination of Gaussian-type orbitals centered on the atomic sites, and the secular equation corresponding to Eq. (1) is diagonalized. In order to make the problem tractable, it is necessary to truncate the secular equation beyond a certain number of shells. It is well known that if the truncation is not performed properly, spurious roots appear which may have energies lying within the band gaps observed in the perfect crystal. Examination of the spatial characteristics of the spurious roots reveals that they result from states residing near the surface of the cluster and, as such, they are often referred to as surface states. For an extremely large cluster, the surface-state contributions to the charge density in the interior of the cluster and the total density of states would be negligible. Therefore, in principle, it is possible to carry out a defect calculation simply by incrementing the number of shells used in constructing the secular equation and monitoring convergence of the defect-level eigenvalues.[24,26] However, in practice, the convergence would be quite slow and it is convenient to truncate the secular equation in a way which quenches the appearance of the surface states completely and reduces the number of shells needed to obtain converged defect eigenvalues. We now discuss this technique.

When we speak of a defect, we implicitly assume that the charge density of the host must eventually converge to that of the perfect crystal far enough from the location of the defect. In other words, it must be possible to describe the ground state of the host-defect system in terms of a set of localized orthogonal atomiclike orbitals, or generalized Wannier functions, which exactly coincide with the perfect-crystal Wannier functions[36] far from the location of the defect. This has been demonstrated explicitly for one-dimensional model defect systems by Kohn *et al.*[37] In order to carry out a defect calculation, we may use as a basis set the Wannier functions which are centered on a given number (Q) of nearest-neighbor atomic shells, plus additional functions which are well localized in the vicinity of the defect. By well localized, we

mean that the overlap between the additional basis functions and the Wannier functions associated with the atoms outside of shell Q must vanish. Suppose this basis set is used to carry out a self-consistent minimization of the energy functional. The convergence must be checked in two ways. First, the density near the shell Q should be compared to the density of the perfect crystal. Secondly, it is necessary to verify that, if additional basis functions, which are slightly more delocalized, are included in the secular equation, the defect-level eigenvalues are unchanged. If either of these tests fail, it is necessary to increase the number of nearest-neighbor shells (Q) used in constructing the secular equation. In addition to the convergence of the defect-level eigenvalues, by using the results of Ref. 38 it is possible to show, in general, that as the number of nearest-neighbor shells (Q) is increased, the occupied bandwidths will increase and converge to the exact result.

Although we have assumed that the perfect-crystal Wannier functions are known, other researchers have noted that other basis sets exist which may be used to properly embed a defect.[13,26,39] In practice, for a cluster containing Q nearest-neighbor shells, it is only necessary to have a basis set which spans the same space as the Wannier functions associated with these shells. This basis set does not necessarily have to be orthonormal. For insulators, it is a good approximation to utilize optimized atomiclike orbitals instead of the Wannier functions, and this is the method that we have adopted. We have compared our optimized atomic orbitals to the perfect-crystal (LiF) Wannier functions to ensure the accuracy of this approximation (see Ref. 25). For semiconductors, it may be very important to use exact Wannier functions to accurately embed a defect. We are in the process of interfacing our Wannier function programs[40] with our defect codes to deal with such systems.

To illustrate the conclusions of this section, we will briefly discuss the numerical aspects of our LCAO cluster calculations. For the LCAO calculations discussed in this paper, we have utilized a very large Gaussian basis set on the origin (the defect site) and the first three nearest-neighbor shells, plus a minimal atomic basis on the origin and first fifteen nearest-neighbor shells of atoms. On the F-center site, six s-type and six p-type single Gaussians with exponents ranging from 2.69 to 0.1 have been included. On the six nearest-neighbor (100) lithium atoms, we have included six s-type single Gaussians with exponents ranging from 1.01 to 0.05, and five p-type Gaussians with exponents ranging from 1.01 to 0.1 On the twelve second-nearest-neighbor (110) fluorine sites we have included two single s-type and p-type Gaussians with exponents of 0.50 and 0.20. On the eight third-nearest-neighbor (111) lithium sites we have included one single s-type Gaussian with an exponent of 0.20. Group theory has been used to block-diagonalize the resulting Hamiltonian and overlap matrices.[35] In Table I we present the valence-band width obtained from our cluster calculation as a function of nearest-neighbor shells. In addition, we have included the lowest and highest eigenvalues as measured relative to the top of the perfect-crystal valence band that has been obtained from a (LCAO) Bloch-function calculation. As expected, the valence-band width increases monotonically with the size of the secular equation. In Table II the a_{1g} and t_{1u} LDA eigenvalues are presented as a function of cluster size. From Table II it is apparent that the eigenvalues are rather well converged at nine nearest-neighbor shells. We have also performed tests to ascertain the adequacy of our basis set. We find that the occupied a_{1g} F-center state is well described by all of the single Gaussians on the nearest-neighbor lithium sites and the five shortest-range Gaussians on the origin. However, for the unoccupied t_{1u} F-center state, the inclusion of all of the Gaussians on the origin and first two nearest-neighbor shells was necessary to obtain a converged t_{1u} eigenvalue. That is, as expected, the t_{1u} state is more extended than the a_{1g} state.

TABLE I. The lowest (bottom) and highest (top) valence-band (Kohn-Sham LDA) eigenvalues as a function of cluster size are shown. Energies are in eV and are given relative to the energy of the Γ_{15}^{v} state obtained from a Bloch-function calculation. The valence-band width as a function of shell size is also given.

Shells	Bottom	Top	Width
4	−2.32	−0.43	1.89
7	−2.62	−0.19	2.43
11	−2.70	−0.14	2.56
15	−2.76	−0.06	2.70
Bloch functions	−3.23	0.00	3.23

B. The muffin-tin Green's-function method

We keep the discussion of the MTGF method brief since a detailed exposition has been given recently.[23] In order to carry out a defect calculation within the framework of the MTGF, it is first necessary to generate a self-consistent band structure and muffin-tin potential for the host crystal. For the host-crystal calculations we have employed the self-consistent (SC) augmented-plane-wave (APW) method.[41] In this method, the crystal charge density and potential is approximated as spherical within a sphere surrounding each atom and taken to be a constant in the region outside of the spheres. Once the

TABLE II. The (Kohn-Sham LDA) eigenvalues of the a_{1g} and t_{1u} states are given as a function of cluster size. Energies are in eV and are measured relative to the energy of the Γ_{15}^{v} state obtained from a Bloch-function calculation. The a_{1g}-t_{1u} splitting δ is also given.

Shells	a_{1g}	t_{1u}	δ
7	4.95	7.25	2.30
9	5.86	10.03	4.17
11	5.86	10.08	4.22
13	5.86	10.11	4.25
15	5.87	10.12	4.25

SC muffin-tin potentials and band structure have been obtained, it is possible to carry out a defect calculation in terms of the Green's-function formalism. The host Green's function, G^0 can be constructed from the APW eigenfunctions using the spectral representation, resulting in

$$G^0(\mathbf{r},\mathbf{r}',E)=\sum_i \frac{\psi_i(\mathbf{r})\psi_i^*(\mathbf{r}')}{E-\varepsilon_i} , \quad (5)$$

ψ_i and ε_i being the wave functions and eigenvalues, respectively. Although the sum is over all the eigenstates, in practice, for performing the necessary Kramers-Kronig inversions the summation can be truncated above a certain large, but finite, cutoff energy. We have varied this cutoff energy to ensure that it is indeed large enough, and have ascertained good convergence. For example, the defect energies obtained using cutoff energies 36.5 and 28.5 eV above the top of the valence band differ by less than 1.1%.

The defect Green's function, G, is related to the host Green's function by a Dyson equation,

$$G=G^0+G^0\Delta V G , \quad (6)$$

where ΔV is the difference between the defect and host-crystal potential [Eq. (3)]. A self-consistent procedure is used to determine the charge density using a contour integration in the complex energy plane (off the real axis). This method is fully described in Ref. 21.

III. DENSITY-FUNCTIONAL RESULTS

A. The perfect crystal

All of our LiF calculations have been carried out with a lattice constant of 7.5954 a.u. We have used both the Kohn-Sham exchange-only[42] and Hedin-Lundqvist[43] (HL) exchange-correlation LDA functions in our calculations. While the latter functional is presumed to be more accurate from the standpoint of the LDA, much of the existing literature on the self-interaction correction has employed the Kohn-Sham exchange-only functional. As such, in this section we discuss Kohn-Sham LDA results also. For the APW calculations we have used muffin-tin radii of 2.39 a.u. for the fluorine ions and 1.4 a.u. for the lithium ions. We find a direct gap ($\Gamma_{15}\rightarrow\Gamma_1$) of 8.55 eV and an occupied F $2p$ bandwidth of 3.21 eV. Owing to the nearly spherical environment about each atomic site, the APW approximation should be particularly good for LiF. In order to estimate the nonspherical corrections, we have interchanged the muffin-tin radii and repeated the calculation leading to a direct band gap of 8.23 eV and a valence-band width of 2.93 eV. While the large-fluorine–small-lithium muffin-tin calculations should be a much better approximation, this confirms that the muffin-tin method should be accurate to a few tenths of an eV or better. The HL band gap and bandwidth obtained from the LCAO formulation are, respectively, 8.90 and 3.19 eV,[44,45] which again indicates that the APW results should be accurate to approximately 0.25 eV. Our LCAO (Ref. 33) Kohn-Sham calculation leads to a band gap of 8.40 eV and a bandwidth of 3.23 eV. Hence, the addition of correlation leads to only a modest increase in the LiF band gap.

There are a variety of experimental estimates of the band gap ranging from 13.6 to 14.6 eV.[46–48] Perhaps the most reliable estimate is 14.2±0.2 eV, which is given in Ref. 49. Regardless, as expected, the LDA-based estimates lead to band gaps which are approximately 40% less than the experimental measurements, in concert with LDA results for other nonmetallic systems.

B. The F center in LiF with the LDA

When a neutral fluorine atom is removed from the LiF host, a neutral F center is created with an electron of a_{1g} (s-like) symmetry occupying the vacancy. In Fig. 1 the perfect-crystal (APW) and F-center (MTGF) local density of states due the central site illustrate that the theory gives a localized a_{1g} state lying within the valence-conduction band gap. In addition to the appearance of a singly occupied a_{1g} state, an unoccupied resonance, largely comprised of t_{1u} (p-like) symmetry, has appeared slightly above the onset of the conduction band. Similar results have been found for the F centers in MgO and CaO using the same approach.[23] With the large fluorine and F-center muffin-tins ($R=2.39$ a.u.), the a_{1g}-t_{1u} splitting (using the center of the t_{1u} resonance peak) is found to be 4.90 eV. Again, to estimate shape corrections we have interchanged the muffin-tin radii and repeated the calculation. While the qualitative placements of the defect levels (with respect to the valence and conduction bands) are the same as those obtained from the former more physical muffin-tin radii, the a_{1g}-t_{1u} splitting is reduced to 4.55 eV. The experimental absorption energy of 5.10 eV is in fair agreement with the Hedin-Lundqvist defect eigenvalue differences. However, we believe that this agreement may be fortuitous since there is little theoreti-

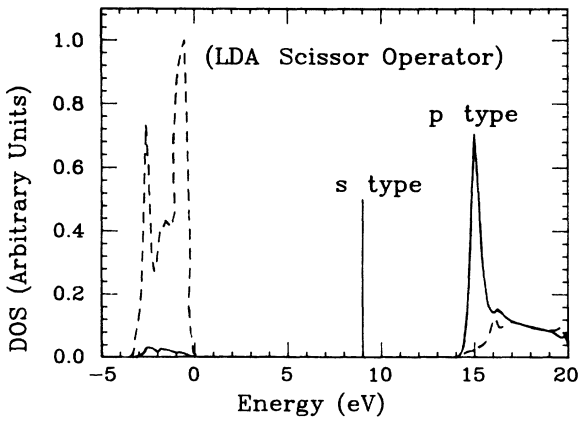

FIG. 1. The MTGF LiF host (dashed curve) and F-center (solid curve) density of states are shown. The resonance above the onset of the conduction band is largely composed of t_{1u} (p-like) symmetry. The occupied state within the valence-conduction band gap is an a_{1g} (s-like) state.

cal justification for expecting that the LDA eigenvalue differences should lead to accurate excitation energies. We have also carried out a SCF (self-consistent-field) Kohn-Sham exchange-only calculation for the F center with our LCAO cluster code. The resulting density of states for a cluster containing all atoms within fifteen nearest-neighbor shells (164 lithium atoms and 140 fluorine atoms) is presented in Fig. 2. Again, we find that the a_{1g} state is between the valence and conduction band and the t_{1u} state lies above the onset of the conduction band. We obtain an a_{1g}-t_{1u} splitting of 4.25 eV. While the LCAO and MTGF methods predict the same qualitative features, the placement of the a_{1g} state, relative to the valence-band edge, obtained from our LCAO codes differs from the MTGF results by approximately 1.0 eV. Although some of this discrepancy is due to the different functionals which have been employed, we believe that most of the deviation is largely attributed to the neglect of charge and potential relaxation beyond the first-nearest-neighbor shells in the MTGF codes.

Although the calculated position of the a_{1g} state is qualitatively correct, it should be noted that the t_{1u} state is incorrectly observed to lie above the onset of the conduction band. Experimentally, it is found that the t_{1u} state lies just below the conduction-band edge with a thermal ionization energy of 0.16 eV.[14] In addition to the experimental information pertaining to the t_{1u} state, a rather general theorem due to Mott and Gurney[50] also indicates that the t_{1u} state should lie below the onset of the conduction band. They showed that, provided the long-range behavior of the effective potential exhibits an asymptotic $-1/r$ limit, a full Rydberg-like continuum should appear below the onset of the conduction band. While the $-1/r$ limit is physically appealing, the LDA effective potential does not exhibit this asymptotic form. Therefore, for a LDA Hamiltonian corresponding to a charge neutral system, there is no formal reason for expecting that the t_{1u} state should lie below the conduction-band edge. Since we are interested in incorporating improvements to the LDA method which enable one to qualitatively predict excited-state energies, it is important to understand the origin of the incorrect placement of the t_{1u} state. That is, before concluding that the incorrect placement of the t_{1u} state is due to an incorrect effective potential, it is appropriate to ascertain whether or not the defect-level locations may be improved by simply "fixing" the perfect-crystal band gap. We now address this question.

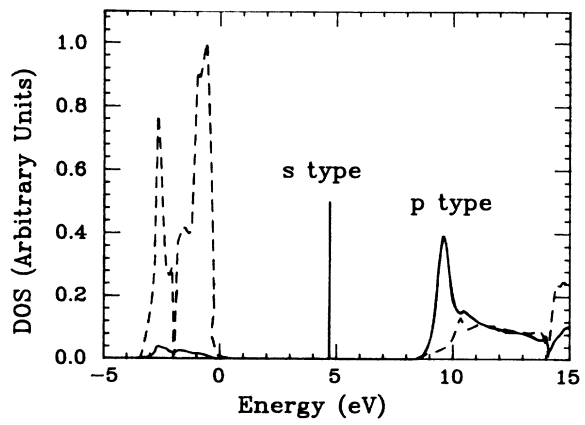

FIG. 2. The MTGF LiF host (dashed curve) and F-center (solid curve) scissored density of states are shown.

C. The scissor operator

In Ref. 23 similar MTGF calculations were carried out on the F center in CaO and MgO. In analogy to the results of the preceding subsection, the occupied a_{1g} states were found to lie between the valence and conduction band and the unoccupied t_{1u} resonances appeared slightly above the onset of the conduction band. Since the LDA leads to substantially reduced band gaps, it is clear that quantitative, and perhaps qualitative, information regarding the location of the defect levels is not possible. In Ref. 23 an *ad hoc* correction to the perfect-crystal band structure was applied prior to the construction of the host-crystal Green's function. In this method, referred to as the scissor operator method, the eigenvalues of the conduction bands are shifted by a constant, Δ, so that the resulting host-perfect-crystal band gap is in agreement with the experiment. That is, the host Green's function is replaced by

$$G^{0'}(\mathbf{r},\mathbf{r}',E)\rightarrow\sum_i \frac{\psi_i^*(\mathbf{r}')\psi_i(\mathbf{r})}{E-\varepsilon_i-\Delta_i}\ , \tag{7}$$

with

$$\Delta_i=\begin{cases}0 & \text{for occupied states}\ , \quad (8)\\ \Delta & \text{for unoccupied states}\ . \quad (9)\end{cases}$$

We note that the resulting Green's function may be associated with the nonlocal Hamiltonian,

$$\left[H_0+\sum_i \Delta_i\,|\,\psi_i\rangle\langle\psi_i\,|-E\right]G^{0'}=-\delta^3(\mathbf{r}-\mathbf{r}')\ . \tag{10}$$

The Hamiltonian corresponding to the scissored Green's function has some intuitive appeal since it builds in orbital-dependent effects in a nonlocal way which is qualitatively similar to the canonical representation of the self-interaction-corrected representation of the local-spin-density Hamiltonian.[32,51] Also, the Hamiltonian and form of the resulting Green's function is reminiscent of the nonlocal mass operator which appears in the many-body self-energy corrections of Pickett and Wang.[52,53]

Once the scissored host Green's function has been introduced, the defect calculation is carried out in the usual way. In Fig. 3 we present the scissored local density of states for the LiF crystal with and without the F center. Aside from the corrected band gap, the qualitative results are the same as that of the straight LDA calculations. There is an occupied a_{1g} state lying in the gap and an unoccupied t_{1u} resonance appearing above the onset of the conduction band. However, the a_{1g}-t_{1u} energy difference has increased to 6.0 eV, substantially higher

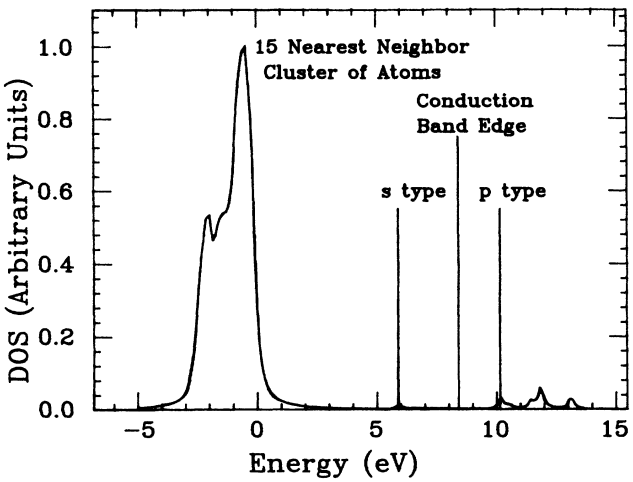

FIG. 3. The LiF F-center (Kohn-Sham) density of states as calculated with a cluster of 140 fluorine atoms and 164 lithium atoms (all atoms within 15 nearest-neighbor shells of the F center).

than the experimental value of 5.1 eV.

Although the modifications of this section have been empirically motivated, the results of this section indicate that, in addition to modifications to the occupied orbital Hamiltonian, corrections to the Hamiltonians observed by the unoccupied defect levels must also be important in order to correctly describe the locations of the defect-induced levels. This is not surprising since, to be rigorous, corrections to LDA should be applied to both the host and defect systems, and there is no *a priori* reason to expect fully satisfactory results from an approach that "fixes" the host band structure only. This subject is discussed in the next section.

IV. LOCALIZED PARTICLE-HOLE EXCITATION THEORY

In the preceding section, we have demonstrated that the present form of LDA is incapable of accurately predicting relative locations of the defect levels in a solid, and we noted that the Mott-Gurney theorem, which guarantees a continuum of bound states below the conduction-band edge, provided the long-range behavior of the effective potential exhibits a $-1/r$ form, is not satisfied in the LDA. In this section we wish to investigate the proper behavior of the correct excited-state potential. For simplicity, in the forthcoming discussions an overall neutral system is assumed. However, the generalizations for charged systems are not difficult. While it might be expected that the potential observed by a localized occupied state should contain a $-1/r$ term outside the range of that state, and while it is physically appealing to assume that the potential observed by an unoccupied level should have the same behavior, it is not immediately clear that this is the case. For example, in the LDA and single-determinant Hartree-Fock formalisms it can be shown that the long-range behavior of the effective potential observed by the unoccupied orbitals vanishes faster than $-1/r$. While neither Hartree-Fock calculations or the LDA are guaranteed to be good for obtaining excited states from ground-state calculations, the excited-state transition-state theory is a fairly well-defined improvement. However, due to the fact that the latter is usually based on the LDA, it can be shown to lead to a long-range potential that also vanishes faster than $-1/r$. An alternative method for extracting information about excited states is to carry out configuration-interaction (CI) calculations, but a simple interpretation is lost since this approach generally leads to a density matrix consisting of many partially occupied orbitals for both the ground and excited states. This makes it difficult to interpret many-body excited states in terms of single-electron excitations. Furthermore, from a practical point of view such calculations are very computer-time-intensive and therefore may not be economically feasible for large systems of scientific interest. Therefore, it is advantageous to search for a computational framework which restores the single-particle picture and is similar to the LDA method. A good single-particle excited-state theory should (at least) exhibit the following characteristics. First, it should be variationally based. Second, the resulting excited state should, by some reasonable definition (preferably in the many-electron sense), be orthogonal to the ground state. Third, from a practical standpoint it would be convenient to predict excited-state energies in terms of orbital eigenvalues or other variationally based, but simple, definitions of orbital energies. In order to gain insight into some of the qualitative characteristics that a "correct" excited-state potential should exhibit, it is first useful to study particle-hole excitations within a more traditional, general quantum-mechanical framework. With this analysis, we will demonstrate that the correct asymptotic behavior of the potential observed by localized excited states should indeed contain a term which behaves as $-1/r$ outside of the range of the active electrons.

A. Particle-hole excitations within a single-determinant theory

In this subsection we discuss a general many-electron variational theory which is particularly well suited for obtaining localized excited states for systems where the highest occupied orbital is well removed in energy from the other occupied orbitals. While the theory is based on many-electron wave functions, in the end a simple single-particle picture for localized excitations emerges.

Suppose that a Hartree-Fock calculation has been carried out on a given system containing N electrons. At SCF we are furnished with a complete set of states which are eigenfunctions of the Fock operator.[54,55] It is useful to divide this space into two orthogonal manifolds. The first manifold contains a representation of the ground-state occupied orbitals, $\{\chi_1,\ldots,\chi_N\}$, and the second manifold contains a representation of the ground-state unoccupied orbitals, $\{\chi_{N+1},\ldots,\chi_M\}$, where M is the dimension of our function space. The indices on these spin orbitals include the spatial and spin quantum numbers. We note that the orbitals in both the occupied and unoccupied manifolds are only determined up to an arbitrary unitary transformation. This fact will be useful shortly. The ground-state Slater determinant will be symbolically represented by,

$$|\,\text{vac}) = A\,|\chi_1,\chi_2,\ldots,\chi_N|\ , \tag{11}$$

where $A\,|\chi_1,\chi_2,\ldots,\chi_N|$ indicates that we are to construct a single Slater determinant composed of the ground-state Hartree-Fock spin orbitals. In Eq. (11) and the forthcoming discussion, we use kets $[\,|\cdots)]$ as a shorthand for many-electron states and pointed kets $[\,|\cdots\rangle]$ for more conventional notation.

The action of the Fock operator (F_g) on an arbitrary spin orbital, $\psi(\mathbf{t})$, is given by

$$F_g\psi(\mathbf{t}) = \left[-\tfrac{1}{2}\nabla^2 + V_{\text{ext}}(\mathbf{r}) + \int d\mathbf{r}'\frac{\rho(\mathbf{r}')}{|\,\mathbf{r}-\mathbf{r}'\,|}\right]\psi(\mathbf{t}) - \sum_j \chi_j(\mathbf{t})\int d\mathbf{t}'\frac{\chi_j^*(\mathbf{t}')\psi(\mathbf{t}')}{|\,\mathbf{r}-\mathbf{r}'\,|}\ , \tag{12}$$

where $\rho(\mathbf{r}')$ is the density due to the occupied manifold. The coordinates $\mathbf{t}$ and $\mathbf{t}'$ represent both spin and spatial coordinates and the integral over $d\mathbf{t}'$ represents an integral over the spatial coordinates and an inner product in spin space. The SCF HF spin orbitals satisfy

$$F_g\chi_i = \begin{cases} \displaystyle\sum_{j=1}^{N}\lambda_{ji}\chi_j, & i \le N \qquad (13) \\ \displaystyle\sum_{j=N+1}^{M}\lambda_{ji}\chi_j, & i > N\ . \qquad (14) \end{cases}$$

We are interested in obtaining the best single Slater determinant for representing the lowest excited state. In order to do this, we wish to construct a trial single Slater determinant which consists of $N-1$ of the ground-state orbitals and one of the excited states. For example, we might consider replacing the orbital χ_k ($k \le N$) by χ_m ($m > N$). This many-electron state is symbolically written as

$$|\chi_k\chi_m) = A\,|\chi_1,\ldots,\chi_{k-1},\chi_m,\chi_{k+1},\ldots,\chi_N|\ , \tag{15}$$

with the ordering of the spin orbitals as implied above. Throughout the remaining discussion we will refer to this as a trial particle-hole excited state (TPHES), with the particle state represented by the ground-state unoccupied orbital (χ_m) and the hole state represented by the ground-state occupied orbital (χ_k). The TPHES is guaranteed to be orthogonal to the ground-state Slater determinant for any choice of particle-hole pair. A fact of equal importance is that, from Brillouin's theorem,[55] the many-electron matrix element between any TPHES and the ground state is guaranteed to vanish, which means that if we were able to carry out a CI calculation using the ground-state Slater determinant and any number of TPHES states there would be no mixing between the TPHES's and the ground-state Slater determinant. As shown in Appendix A, the expectation value of a TPHES is given by

$$E(\chi_k\chi_m) = (\chi_k\chi_m\,|\,H\,|\,\chi_k\chi_m) \tag{16a}$$

$$= E(\text{vac}) + \langle\chi_m\,|\,F_g\,|\,\chi_m\rangle - \langle\chi_k\,|\,F_g\,|\,\chi_k\rangle - \langle\chi_k\chi_m\,|\,(1/r_{12})\,|\,\chi_k\chi_m\rangle + \langle\chi_k\chi_m\,|\,(1/r_{12})\,|\,\chi_m\chi_k\rangle\ . \tag{16b}$$

In Eq. (16a), H is the many-electron Hamiltonian which is given by

$$H = \sum_{i=1}^{N} -\tfrac{1}{2}\nabla_i^2 + V_{\text{ext}}(\mathbf{r}_i) + \tfrac{1}{2}\sum_{i,j}{}'\frac{1}{r_{ij}}\ , \tag{17}$$

and $(\chi_k\chi_m\,|\,H\,|\,\chi_k\chi_m)$ is the energy of the (many-electron) particle-hole state $|\,\chi_k\chi_m)$. In Eq. (16b), F_g is the ground-state Fock operator of Eq. (12) and $\langle\chi\,|\,F_g\,|\,\chi\rangle$ is the energy associated with the single-particle state $|\,\chi\rangle$. In Eq. (16b) we have adopted Slater's notation for the two-electron integrals.[54] That is,

$$\langle\chi_k\chi_l\,|\,(1/r_{12})\,|\,\chi_m\chi_n\rangle \equiv \int d\mathbf{t}_1 d\mathbf{t}_2 (1/r_{12})\chi_k^*(t_1)\chi_l^*(\mathbf{t}_2)\chi_m(\mathbf{t}_1)\chi_n(\mathbf{t}_2)\ , \tag{18}$$

where $\mathbf{t}_1$ and $\mathbf{t}_2$, and their integrals, have been defined above. The constant E(vac) corresponds to the energy, (vac $|\,H\,|$ vac), of the many-electron ground-state Slater determinant.

Within this framework, the best approximation to the lowest excited state is clearly that particle-hole pair which leads to a minimum excited-state energy. Alternatively, since E(vac) is a constant, we may minimize the difference between the excited-state and ground-state total energy, which is given by

$$\Delta E = \langle\chi_m\,|\,F_g\,|\,\chi_m\rangle - \langle\chi_k\,|\,F_g\,|\,\chi_k\rangle - \langle\chi_k\chi_m\,|\,(1/r_{12})\,|\,\chi_k\chi_m\rangle + \langle\chi_k\chi_m\,|\,(1/r_{12})\,|\,\chi_m\chi_k\rangle\ . \tag{19}$$

For example, for a given representation of the occupied and unoccupied manifolds, we might estimate the minimum of ΔE by searching through $N(M-N)$ particle-hole pairs and finding the pair which minimizes ΔE. This would certainly be a tedious endeavor and it would lead to an excitation energy which would be dependent on the original choice of representation. A better method is to, in analogy to Koopmans's theorem for ionization energies,[56,57] exploit the unitary invariance of the Fock operator and note that we may write the energy difference of the most general TPHES as

$$\Delta E = \langle C\,|\,F_g\,|\,C\rangle - \langle V\,|\,F_g\,|\,V\rangle - \langle VC\,|\,(1/r_{12})\,|\,VC\rangle + \langle VC\,|\,(1/r_{12})\,|\,CV\rangle\ , \tag{20}$$

where C and V are, respectively, *arbitrary* normalized

linear combinations of the unoccupied and occupied orbitals. In other words, for any given normalized functions C and V which are constrained to lie in the appropriate manifolds, it is possible to find orbital representations of the occupied and unoccupied manifolds for which C and V represent a particle-hole pair. Hence, it is evident that the best single-determinant particle-hole excited state may be found by minimizing Eq. (20) subject to the constraints

$$V=\sum_{j=1}^{N} a_j^V \chi_j \ , \tag{21}$$

$$C=\sum_{j=N+1}^{M} a_j^C \chi_j \ , \tag{22}$$

$$\langle V \mid V\rangle=\langle C \mid C\rangle=1 \ , \tag{23}$$

with the constraint $\langle V \mid C\rangle=0$ satisfied by construction. Note that the unitary transformation that takes us from the original $\{\chi\}$ spin-orbital basis defines N or $M-N$ new occupied or unoccupied states, respectively, of which $\mid V\rangle$ and $\mid C\rangle$ are particular states. That is, the expansion coefficients for the particle (hole) states may be viewed as one row of a unitary matrix which operates on the occupied (unoccupied) manifold. In order to find the best particle-hole pair, we apply the variational principle to Eqs. (20)–(23) which, as outlined in Appendix A, leads to the following secular equations,

$$\langle \chi_l \mid F_g-\Delta_V \mid C\rangle=\varepsilon_C\langle \chi_1 \mid C\rangle \quad (l>N) \ , \tag{24}$$

$$\langle \chi_l \mid F_g+\Delta_C \mid V\rangle=\varepsilon_V\langle \chi_1 \mid V\rangle \quad (l\leq N) \ , \tag{25}$$

$$\Delta_V \mid C\rangle\equiv\int d\mathbf{r}'\frac{\rho_V(\mathbf{r}')}{\mid \mathbf{r}-\mathbf{r}'\mid}\mid C\rangle-\mid V\rangle\int d\mathbf{t}'\frac{V^*(\mathbf{t}')C(\mathbf{t}')}{\mid \mathbf{r}-\mathbf{r}'\mid} \ , \tag{26}$$

and a similar equation for $\Delta_C \mid V\rangle$ with V and C interchanged. We note that when the operator $F_g-\Delta_V$ operates on an arbitrary $\psi(t)$, the electron-electron contributions may be written as

$$\sum_{i=1}^{N-1}\psi(\mathbf{t})\int d\mathbf{r}'\frac{\phi_i^*(\mathbf{t})\phi_i(\mathbf{t}')}{\mid \mathbf{r}-\mathbf{r}'\mid}-\phi_i(\mathbf{t})\int d\mathbf{t}'\frac{\phi_i^*(\mathbf{t}')\psi(\mathbf{t}')}{\mid \mathbf{r}-\mathbf{r}'\mid} \ , \tag{27}$$

where the $N-1$ ϕ_i orbitals (which together with V complete the new occupied manifold) are orthogonal to V. Hence we see that there is no explicit V dependence of the operator $F_g-\Delta_V$.

Analysis of the above equations reveals several interesting features. Equation (24) has the attractive physical interpretation that the excited-state electron, C, neither Coulomb- nor exchange-interacts with the hole state. Further, it is easily verified that if V is localized within some region of space, outside of this region, the $\Delta_V \mid C\rangle$ term in Eqs. (24) and (26) behaves as

$$\Delta_V \mid C\rangle\rightarrow(1/r)\mid C\rangle \ . \tag{28}$$

In Appendix B we demonstrate that the term $F_g \mid C\rangle$ in Eq. (24) has no $(1/r)$-type contribution. Therefore, the correct excited-state Hamiltonian, $F_g-\Delta_V$, contains a $-1/r$ contribution outside the range of the hole state.

Analysis of Eq. (25) indicates that the hole-state electron "sees" a potential which contains no net $1/r$ contributions. That is, as discussed in Appendix B, outside the range of the hole state the exchange part of the Fock operator contributes a $-1/r$ term to the effective potential which is exactly cancelled by a $1/r$ contribution outside the range of the excited-state wave function. However, it is interesting to note that the energy difference is conveniently reexpressed as

$$\Delta E=\langle C \mid F_g-\Delta_V \mid C\rangle-\langle V \mid F_g-\Delta_V \mid V\rangle \ . \tag{29}$$

The above equation follows from Eqs. (20) and (26) and the fact that $\Delta_V \mid V\rangle=0$. The above analysis indicates that once we are given C and V, the sensible definition of the orbital energies is the expectation value of the operator $F_g-\Delta_V$. In order to test the conclusions of this subsection, it is useful to point out that our particle-hole excited-state formalism reduces to the Hartree-Fock Koopmans's theorem under certain conditions. That is, for a finite system, we note that if the hole state is taken to be the least negative canonical orbital, and the particle state is taken to be an orthogonalized plane wave, this particle-hole pair will satisfy Eqs. (24) and (25). Further, from Eq. (29), the excited energy reduces to

$$\Delta E=\tfrac{1}{2}k^2-\langle V \mid F_g \mid V\rangle \ , \tag{30}$$

which is the difference between the least negative ground-state eigenvalue and the kinetic energy of the hole state. If the hole state is placed in a state with zero kinetic energy ($k=0$), it is evident that an apparent single-electron ionization between N- and $(N-1)$-electron ground states may also be reconciled as a stationary particle-hole N-electron excited state. However, we note that this stationary particle-hole N-electron state seldom (if ever for physical systems) coincides with the lowest N-electron particle-hole excited state.

We now wish to compare the single-particle energies that have been defined from the expectation value of the particle-hole energy operator $F_g-\Delta_V$ to the single-particle energies that were used in the preceding section, where we have used the expectation value of the ground-state LDA Hamiltonian to define single-particle energies. For localized excitations, the LDA Hamiltonian differs (qualitatively) from the particle-hole energy operator in two ways. First, the LDA Hamiltonian explicitly depends on all of the ground-state occupied orbitals, including the hole electron. Second, outside the range of the hole wave function, the LDA Hamiltonian does not contain a $-1/r$ term, whereas the particle-hole energy operator does. However, if we accept the assertion that the expectation values of the LDA Hamiltonian constitute a reasonable first approximation to the expectation value of the particle-hole energy operator, we should consider appending an additional term to the LDA Hamiltonian which either exactly or approximately removes the V dependence and restores the correct long-range $1/r$ behavior. A candidate for such a term is the SIC potential

associated with the hole-state charge density, which is given by

$$\Delta V^{\mathrm{SIC}} = -\int d\mathbf{r}' \frac{\rho_V(\mathbf{r}')}{|\mathbf{r}-\mathbf{r}'|} - V_{\mathrm{xc}}[\rho_V, 0] \ . \tag{31}$$

The above correction leads to an effective Hamiltonian which exhibits the exact $1/r$ behavior and correct electronic Coulomb terms. In addition, it approximately cancels the hole density-dependent exchange-correlation terms. In the next section we apply this correction to the F center in LiF. However, before doing so, we wish to point out why these arguments are valid for localized (no near degeneracies) excitations but not for delocalized (near degeneracies) excitations.

If one attempts to employ the arguments of this subsection to obtain delocalized excitation energies, care must be exercised since there are conceptual pitfalls which one may run into. In fact, for a perfect crystal, if one assumes that two Bloch states are candidates for a particle-hole pair, it is apparent that both Δ_V and Δ_C would vanish as $1/N$ (N is the number of unit cells). This leads to the incorrect conclusion that the Hartree-Fock band gap is correct. There are two reasons why this is a faulty conclusion. First, even though a particle-hole pair constructed from Bloch states leads to a stationary excited-state energy, it does not guarantee that this energy is a minimum. Indeed localized excitonic levels generally correspond to the lowest excited states in the crystal. Further, if it did turn out that the excitonic levels were not the minimum in energy, it is still true that there would be many (of order N) nearly degenerate particle-hole Bloch states of the same symmetry, and it is cases of this sort where single-determinant theory breaks down and configuration interaction is necessary. Therefore, generalizing the above arguments to delocalized excitations is still an open question.

V. THE LIF F CENTER WITH THE SELF-INTERACTION CORRECTION

In the preceding section we used many-body arguments to investigate the proper behavior of the excited-state Hamiltonian. We have demonstrated that localized excited-state energies may be found by defining our single-particle energies for the active electrons to be expectation values of a variationally derived particle-hole energy operator which is qualitatively similar to the self-interaction-corrected LDA Hamiltonian. It should be noted that, in applications to excited atomic states, a similar conclusion has been drawn by Harrison *et al.*,[30] using arguments based on the assumption that the self-interaction corrected local-spin density (SIC-LSD) energy functional is equally valid for the excited state as well as the ground state. Further, they have presented numerical evidence for approximately 80 first-row transitions, which indicates that the SIC-LSD Hamiltonian does indeed lead to accurate excited-state energies.

Therefore, in this section we shall apply the SIC-LSD to both the ground and excited states of the F center in LiF. Since numerous articles devoted to the SIC-LSD formalism have appeared in the literature,[26–32,51] we will limit our discussion of the problem to the localized levels in the LiF F center.

With the inclusion of SIC to the LSD energy functional, the electronic contribution to the total energy is given by

$$E_t = \sum_{\sigma,\lambda,s,n,q} \langle \phi^{\lambda s}_{\sigma nq}(\mathbf{r}-\mathbf{R}^{\lambda}_s) | -\tfrac{1}{2}\nabla^2 + V_{\mathrm{ext}} | \phi^{\lambda s}_{\sigma nq}(\mathbf{r}-\mathbf{R}^{\lambda}_s)\rangle + \tfrac{1}{2}\int d\mathbf{r}\int d\mathbf{r}' \frac{1}{|r-r'|}\rho(\mathbf{r})\rho(\mathbf{r}') + \int dr \rho(\mathbf{r})\varepsilon_{\mathrm{xc}}(\rho_\uparrow,\rho_\downarrow)$$
$$- \sum_{\sigma,\lambda,s,n,q} \tfrac{1}{2}\int d\mathbf{r}\int d\mathbf{r}' \frac{1}{|r-r'|}\rho^{\lambda s}_{\sigma nq}(\mathbf{r}-\mathbf{R}^{\lambda}_s)\rho^{1s}_{\sigma nq}(\mathbf{r}-\mathbf{R}^{\lambda}_s) + \int d\mathbf{r}' \rho^{\lambda s}_{\sigma nq}(\mathbf{r}-\mathbf{R}^{\lambda}_s)\varepsilon_{\mathrm{xc}}(\rho^{\lambda s}_{\sigma nq}, 0) \ . \tag{32}$$

The first three terms of Eq. (32) represent the usual LSD total energy. The remaining SIC term is constructed from the orthonormal local-orbital densities $\rho^{\lambda s}_{\sigma nq}$ and approximately corrects for any spurious self-interaction terms in the LSD energy functional. The orbital $\phi^{\lambda s}_{\sigma nq}$ has spin index σ, band index n, subband index q, shell index σ, and site index s. These orbitals are localized about their respective atomic sites and coincide with the perfect crystal SIC-LSD Wannier functions far from the F center. By demanding that Eq. (32) is minimized subject to the orthonormality constraints

$$\langle \phi^{\lambda s}_{\sigma nq}(\mathbf{r}-\mathbf{R}^{\lambda}_s) | \phi^{\lambda' s'}_{\sigma n' q'}(\mathbf{r}-\mathbf{R}^{\lambda'}_{s'})\rangle = \delta_{nn'}\delta_{qq'}\delta_{ss'}\delta_{\lambda\lambda'} \ , \tag{33}$$

it is found that the orbitals which minimize the total energy satisfy coupled Schrödinger and localization equations which are, respectively, given by[32]

$$(H_{0\sigma} + V^{\mathrm{SIC}}_{i\sigma})\phi_{i\sigma} = \sum_j \varepsilon_{ji}\phi_{j\sigma} \ , \tag{34}$$

$$\langle \phi_{j\sigma} | V^{\mathrm{SIC}}_{j\sigma} - V^{\mathrm{SIC}}_{i\sigma} | \phi_{i\sigma}\rangle = 0 \ . \tag{35}$$

In the above equation the single indices i and j represent the multi-indices λ,s,n,q and λ',s',n',q', respectively.

The localization equations ensure that the SCF Lagrange-multiplier matrix is Hermitian. Therefore, it is possible to diagonalize the Lagrange-multiplier matrix and rewrite the SCF equations in terms of the canonical orbitals according to

$$(H_{0\sigma} + \Delta V^{\mathrm{SIC}}_{n\sigma})\psi_{n\sigma} = \lambda_{n\sigma}\psi_{n\sigma} \ . \tag{36}$$

Here we note that $\Delta V^{\mathrm{SIC}}_{n\sigma}$ is the canonical representation of the SIC potential, which, for a localized state, is extremely close to the localized representation of the SIC

potential given in Eq. (31). We stress the fact that, even with the orbital dependence of the above Hamiltonian, the resulting canonical orbitals form an orthonormal set and are indeed eigenfunctions of their respective Hamiltonians. Further, it has been shown in a previous paper that to first order the eigenvalue corresponds to an ionization energy and that the second-order corrections are quite small.[32]

In practice, carrying out the above algorithm would be rather cumbersome. Hence, we have introduced some simplifications which have been thoroughly explored in atomic and molecular calculations[32,51,58] and are known to lead to accurate results. The first simplification is to ignore the localization equations between different bands. Secondly, in carrying out the SIC-LSD calculation we have limited the crystal bands to lie in the same function space as the corresponding LSD bands. With these simplifications, the defect levels may be found by first carrying out a LSD calculation and then finding a self-consistent solution to the following equation,

$$\Theta(H_0+V_{a_{1g}}^{\mathrm{SIC}})\Theta\psi_{a_{1g}}=\varepsilon_{a_{1g}}\psi_{a_{1g}}\ , \tag{37}$$

$$\Theta=1-\sum_{i=1}^{\text{occ-1}}|\phi_i\rangle\langle\phi_i|\ . \tag{38}$$

In the above equation, H_0 is the usual LSD Hamiltonian, $V_{a_{1g}}^{\mathrm{SIC}}$ is the SIC potential due to the F-center electron, and Θ is an operator which projects out the other occupied crystal states. For a more complete discussion, see Ref. 32.

A. Results

In Fig. 4 we compare the Kohn-Sham LDA defect levels to the Kohn-Sham SIC-LSD defect levels relative to the conduction band. In presenting the data in Fig. 4, we have assumed that the onset of the conduction band is correctly described by the LDA and that there are no SIC-like or self-energy corrections for the delocalized conduction-band states. Justifications for this approximation, which are based on the *assumption* that the SIC-LSD energy functional is equally valid for both the ground and excited states, have been discussed elsewhere[31,58] and will not be repeated here since we are primarily interested in the defect. However, we note that recent work on applications of the SIC-LSD to the alkali fluorides, alkali chlorides, and solid argon[31,45] indicate that the resulting perfect-crystal band gap is improved when this approximation for the conduction band is employed. From Fig. 4 it is apparent that the addition of the SIC has pulled the defect levels to lower energies. The Kohn-Sham a_{1g}-t_{1u} eigenvalue difference is found to be 4.25 eV. With the addition of the SIC, the eigenvalue difference increases to 5.1 eV, which is in perfect agreement with the experimental measurement of 5.1 eV. While this agreement is extremely good, our calculations may be uncertain to about 0.1 eV and we note that the experimental absorption is quite broad with a zero-point half-width of 0.6 eV. Further, preliminary calculations indicate that the effects of lattice relaxation will change the eigenvalue difference by approximately 0.1 eV. In addition to an improved excitation energy, Fig. 4 illustrates that inclusion of the SIC potential leads to a better qualitative picture of the location of the defect levels relative to the conduction band. As discussed above, the LDA results lead to an occupied a_{1g} state in the gap, and an unoccupied t_{1u} state above the onset of the conduction band, which is in disagreement with experiment and the Mott-Gurney theorem, which asserts that the t_{1u} state should lie below the onset of the conduction band. From Fig. 4 it is evident that, within the framework of the SIC-LSD formalism, both the a_{1g} and t_{1u} states are found below the onset of the conduction band. The defect levels are indeed quite localized with root-mean-square radial moments, $(\langle\psi|r^2|\psi\rangle)^{1/2}$, of 3.01 and 4.20 a.u. for the a_{1g} and t_{1u} states, respectively. Aside from the occurrence of a t_{1u} gap state, additional unoccupied states have been pulled below the onset of the conduction band, which indicates that the Mott-Gurney continuum is being partially restored within the SIC-LSD LCAO cluster method. Due to the finite basis, it is not possible to find the entire Mott-Gurney continuum, but it is encouraging to see that additional levels are appearing as the cluster size increases. Experimentally, it is found that an electron in the t_{1u} state has a thermal ionization energy of 0.16 eV, which is quite a bit smaller than the 3.5-eV location of this state below the conduction-band edge found in our work (see Fig. 4). There are several possible reasons for this discrepancy. First, if the F-center electron occupies a t_{1u} state, the point-group state is reduced, so there may be a rather large Jahn-Teller distortion after the a_{1g}-t_{1u} excitation takes place. Indeed, while we are unaware of any data for the LiF Stokes shift, for 14 other alkali-halide F centers such shifts are typically found to be 1.0 eV,[14] which indicates a great deal of relaxation of the excited state. Another possibility, is that SIC-like or self-energy shifts for the conduction band may not be completely negligible.

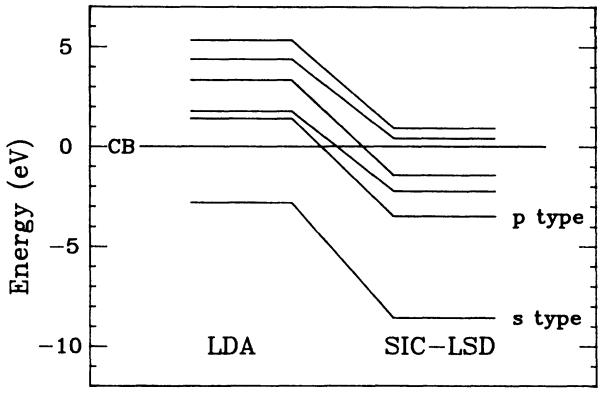

FIG. 4. The effect of the self-interaction correction on the defect levels is shown. Energies are given relative to the LDA conduction-band edge.

VI. CONCLUSION

In this paper we have studied the F center in LiF using both the MTGF formulation and the LCAO cluster

method. Within the framework of the LDA, we find that the qualitative placement of the occupied levels of the host-defect system are correctly described. However, the LDA predicts that there is only one defect level within the valence-conduction band gap, which is in disagreement with both experiment and the Mott-Gurney theorem. We have utilized a many-electron variational argument to extract information about particle-hole excited states and find that, within a single-determinant theory, the excited-particle state should neither Coulomb or exchange-interact with the removed hole density. A direct manifestation of this fact is that the long-range behavior of the effective potential for the excited-particle state should behave as $-1/r$ for charge-neutral systems. In addition to information about effective Hamiltonians, a logical definition for "single-particle energies" emerges from our arguments. We note that this definition is qualitatively, and nearly quantitatively, the same as a previous definition for particle-hole excited states which has been utilized for SIC-LSD atomic calculations. Hence, we have included the SIC in our F-center calculation and find that the resulting a_{1g}-t_{1u} transition energy is in very good agreement with experiment. Further, the SIC-LSD calculation correctly predicts that the t_{1u} state lies below the onset of the conduction band, and, within the constraints of our finite basis, begins to build in the Mott-Gurney continuum. While the agreement between our SIC-LSD LCAO cluster calculations and experiment is quite encouraging, the effects of ground-state lattice relaxation and excited-state Jahn-Teller distortion should be included to obtain a full picture of the excitation process.

ACKNOWLEDGMENTS

We thank W. E. Pickett, J. G. Harrison, and C. C. Lin for helpful discussions. This work was supported in part by the Office of Naval Research. One of us (M.R.P.) thanks the National Research Council for partial support.

APPENDIX A

In this appendix we provide some of the details which lead to Eqs. (16) and (20) and outline the variational arguments which lead to Eqs. (24)–(26). Using the notation of Sec. IV A, the Hartree-Fock energy of the vacuum state may be written as[54]

$$\begin{aligned} E(\text{vac}) &= (\text{vac}\,|\,H\,|\,\text{vac}) \\ &= \sum_{i=1}^{N} \langle \chi_i\,|\,-\tfrac{1}{2}\nabla^2+V_{\text{ext}}\,|\,\chi_i\rangle \\ &\quad +\tfrac{1}{2}\sum_{i,j}^{N}[\langle \chi_i\chi_j\,|\,(1/r_{12})\,|\,\chi_i\chi_j\rangle \\ &\quad -\langle \chi_i\chi_j\,|\,(1/r_{12})\,|\,\chi_j\chi_i\rangle]\,. \end{aligned} \tag{A1}$$

To derive Eq. (16) it is useful to introduce the following notation,

$$S_p=\sum_{\substack{i=1\\(i\neq k)}}^{N}\langle \chi_i\,|\,-\tfrac{1}{2}\nabla^2+V_{\text{ext}}\,|\,\chi_i\rangle\,, \tag{A2}$$

$$\begin{aligned} T_p=\tfrac{1}{2}\sum_{\substack{i=1\\(i\neq k)}}^{N}\sum_{\substack{j=1\\(i\neq k)}}^{N}&[\langle \chi_i\chi_j\,|\,(1/r_{12})\,|\,\chi_i\chi_j\rangle \\ &-\langle \chi_i\chi_j\,|\,(1/r_{12})\,|\,\chi_j\chi_i\rangle]\,, \end{aligned} \tag{A3}$$

where S_p and T_p, respectively, refer to the single-electron and two-electron contributions to the total energy due to the passive orbitals (those that are not involved in the excitation). The energy of the vacuum state may then be rewritten as

$$E(\text{vac})=S_p+T_p+\langle \chi_k\,|\,F_g\,|\,\chi_k\rangle\,, \tag{A4}$$

where F_g is defined by Eq. (12). In a similar way we may decompose the trial excited state as

$$E(\chi_k,\chi_m)=S_p+T_p+\langle \chi_m\,|\,F_x\,|\,\chi_m\rangle\,. \tag{A5}$$

In the above equation, F_x is the Fock operator for the excited state, which differs from F_g in that all occurrences of χ_k are replaced by χ_m. In other words,

$$\begin{aligned} \langle \chi_m\,|\,F_x\,|\,\chi_m\rangle &= \langle \chi_m\,|\,F_g\,|\,\chi_m\rangle \\ &\quad -\langle \chi_k\chi_m\,|\,(1/r_{12})\,|\,\chi_k\chi_m\rangle \\ &\quad +\langle \chi_k\chi_m\,|\,(1/r_{12})\,|\,\chi_m\chi_k\rangle\,. \end{aligned} \tag{A6}$$

By substituting Eq. (A6) into Eq. (A5) and subtracting Eq. (A4), we obtain

$$\begin{aligned} E(\chi_k,\chi_m)=E(\text{vac})&+\langle \chi_m\,|\,F_g\,|\,\chi_m\rangle-\langle \chi_k\,|\,F_g\,|\,\chi_k\rangle \\ &-\langle \chi_k\chi_m\,|\,(1/r_{12})\,|\,\chi_k\chi_m\rangle \\ &+\langle \chi_k\chi_m\,|\,(1/r_{12})\,|\,\chi_m\chi_k\rangle\,, \end{aligned} \tag{A7}$$

which is identical to Eq. (16). We now proceed with the derivations of Eqs. (24)–(26).

We start by reiterating that the energy of an arbitrary TPHES is given by

$$\begin{aligned} \Delta E=&\langle C\,|\,F_g\,|\,C\rangle-\langle V\,|\,F_g\,|\,V\rangle-\langle VC\,|\,(1/r_{12})\,|\,VC\rangle \\ &+\langle VC\,|\,(1/r_{12})\,|\,CV\rangle\,, \end{aligned} \tag{A8}$$

where C and V are given by Eqs. (21)–(23). The first variation of ΔE is given by

$$\begin{aligned} \delta(\Delta E)=[&\langle \delta C\,|\,(F_g-\Delta_V)\,|\,C\rangle \\ &-\langle \delta V\,|\,(F_g+\Delta_C)\,|\,V\rangle]+\text{c.c.}\,, \end{aligned} \tag{A9}$$

with $\Delta_V\,|\,C\rangle$ and $\Delta_C\,|\,V\rangle$ defined according to Eq. (26). Now, if C and V minimize Eq. (A8), it follows that Eq. (A9) must vanish. Since δC and δV are arbitrary variations which conserve the constraints imposed by Eqs. (21)–(23), we must have

$$\delta V=\sum_{j=1}^{N}\delta a_j^V\chi_j\ , \tag{A10}$$

$$\delta C=\sum_{j=N+1}^{M}\delta a_j^C\chi_j\ , \tag{A11}$$

$$\langle\delta V\mid V\rangle=\langle\delta C\mid C\rangle=0\ . \tag{A12}$$

Owing to Eq. (A12), we may rewrite Eq. (A9) as

$$\delta(\Delta E)=[\langle\delta C\mid(F_g-\Delta_V-\varepsilon_C)\mid C\rangle - \langle\delta V\mid(F_g+\Delta_C-\varepsilon_V)\mid V\rangle]+\text{c.c.}=0\ . \tag{A13}$$

Substituting Eqs. (A10) and (A11) into Eq. (A13) and requiring that each coefficient of δa_j^V and δa_j^C vanish independently leads to Eqs. (24) and (25).

APPENDIX B

We have been discussing systems which are charge neutral. Hence the nuclear Coulomb potential is exactly screened by the electronic Coulomb potential, so any asymptotic $-1/r$ contributions will be due to the exchange operator whose action on an arbitrary function ψ is summarized by

$$F_g^x\psi(\mathbf{t})=-\sum_j\chi_j(\mathbf{t})\int dt'\frac{\chi_j^*(\mathbf{t}')\psi(\mathbf{t}')}{|\mathbf{r}-\mathbf{r}'|}\ . \tag{B1}$$

If all of the functions χ_j are localized within a given region of space, or if ψ is localized within a given region of space, outside that region Eq. (B1) may be approximated as

$$F_g^x\psi(\mathbf{t})\rightarrow-\frac{1}{r}\sum_j|\chi_j\rangle\langle\chi_j\mid\psi\rangle+O(1/r^2)\ . \tag{B2}$$

Hence it is apparent that if ψ lies entirely in the unoccupied manifold, $\langle\chi_j\mid\psi\rangle=0$, and there is no long-range $1/r$ behavior. In contrast, if ψ lies entirely in the occupied manifold, the above expression reduces to

$$F_g^x\psi(\mathbf{t})\rightarrow-\frac{1}{r}\psi(\mathbf{r})+O(1/r^2)\ . \tag{B3}$$

[1]R. K. Dawson and D. Pooley, Phys. Status Solidi **35**, 95 (1969).
[2]U. M. Grassano, G. Margitondo, and R. Rosei, Phys. Rev. B **2**, 3319 (1970).
[3]H. Rabin and M. Reich, Phys. Rev. **135**, A101 (1964).
[4]H. F. Ivey, Phys. Rev. **72**, 341 (1947).
[5]B. S. Gourary and F. J. Adrian, Phys. Rev. **105**, 1180 (1957).
[6]R. F. Wood and H. W. Joy, Phys. Rev. **136**, A451 (1964).
[7]R. H. Bartran, A. M. Stoneham, and P. Gash, Phys. Rev. **176**, 1014 (1968).
[8]R. C. Chaney, Phys. Rev. B **14**, 4578 (1976).
[9]R. C. Chaney and C. C. Lin, Phys. Rev. B **13**, 843 (1976).
[10]J. N. Murrel and J. Tennyson, Chem. Phys. Lett. **69**, 212 (1980).
[11]C. H. Leung and K. S. Song, Can. J. Phys. **58**, 412 (1980).
[12]J. Tennyson and J. N. Murrel, Mol. Phys. **42**, 297 (1981).
[13]A. Y. Kung, A. B. Kunz, and J. M. Vail, Phys. Rev. B **26**, 3352 (1982).
[14]W. B. Fowler, *Physics of Color Centers* (Academic, New York, 1968).
[15]A. Zunger and M. L. Cohen, Phys. Rev. B **18**, 5449 (1978).
[16]R. A. Heaton and C. C. Lin, Phys. Rev. B **22**, 3629 (1980).
[17]C. S. Wang and B. M. Klein, Phys. Rev. B **24**, 3417 (1981).
[18]C. S. Wang and B. M. Klein, Phys. Rev. B **24**, 3393 (1981).
[19]R. Zeller and P. H. Dederichs, Phys. Rev. Lett. **42**, 1713 (1979).
[20]R. Podloucky, R. Zeller, and P. H. Dederichs, Phys. Rev. B **22**, 5777 (1980).
[21]R. Zeller, J. Deutz, and P. H. Dederichs, Solid State Commun. **44**, 993 (1982).
[22]P. J. Braspenning, R. Zeller, A. Lodder, and P. H. Dederichs, Phys. Rev. B **29**, 703 (1984).
[23]B. M. Klein, W. E. Pickett, L. L. Boyer, and R. Zeller, Phys. Rev. B **35**, 5802 (1987).
[24]W. P. Menzel, K. Mednick, C. C. Lin, and C. F. Dorman, J. Chem. Phys. **63**, 4708 (1975).
[25]M. R. Pederson and B. M. Klein, Mater. Sci. Forum (to be published).
[26]R. A. Heaton, J. G. Harrison, and C. C. Lin, Phys. Rev. B **31**, 1077 (1985).
[27]I. Lindgren, Int. J. Quantum Chem. Symp. **5**, 411 (1971).
[28]J. P. Perdew, Chem. Phys. Lett. **64**, 127 (1979).
[29]J. P. Perdew and A. Zunger, Phys. Rev. B **23**, 5048 (1981).
[30]J. G. Harrison, R. A. Heaton, and C. C. Lin, J. Phys. B **16**, 2079 (1983).
[31]R. A. Heaton, J. G. Harrison, and C. C. Lin, Phys. Rev. B **28**, 5992 (1983); R. A. Heaton and C. C. Lin, J. Phys. C **17**, 1853 (1984).
[32]M. R. Pederson, R. A. Heaton, and C. C. Lin, J. Chem. Phys. **80**, 1972 (1984); **82**, 2688 (1985).
[33]S. C. Erwin, R. A. Heaton, and C. C. Lin, in BANDAID: A Software Package for the Calculation of Electronic Structure by the LCAO Method (University of Wisconsin Software Development and Distribution Center, 1986).
[34]E. U. Condon and G. H. Shortley, *The Theory of Atomic Spectra* (Cambridge University Press, New York, 1967).
[35]F. A. Cotton, *Chemical Applications of Group Theory* (Wiley-Interscience, New York, 1971).
[36]G. H. Wannier, Phys. Rev. **52**, 191 (1937).
[37]W. Kohn and J. R. Onffroy, Phys. Rev. B **8**, 2485 (1973); J. J. Rehr and W. Kohn, *ibid.* **9**, 1981 (1974).
[38]J. K. L. MacDonald, Phys. Rev. **41**, 830 (1933).
[39]A. B. Kunz and D. L. Klein, Phys. Rev. B **17**, 4614 (1978).
[40]M. R. Pederson and C. C. Lin, Phys. Rev. B **35**, 2273 (1987-I).
[41]L. F. Mattheiss, J. H. Wood, and A. C. Switendick, in *Methods in Computational Physics,* edited by B. Alder, S. Fernbach, and M. Rotenberg (Academic, New York, 1968), Vol. 8.
[42]W. Kohn and L. J. Sham, Phys. Rev. **140**, A1133 (1965).
[43]L. Hedin and B. I. Lundqvist, J. Phys. C **4**, 2064 (1971).
[44]S. C. Erwin (private communication).
[45]S. C. Erwin and C. C. Lin, J. Phys. C (to be published).
[46]D. M. Roessler and W. C. Walker, J. Chem. Solids **28**, 1407 (1967).
[47]M. Piacentini, D. W. Lynch, and C. G. Olson (unpublished);

Phys. Rev. Lett. **35**, 1658 (1976).
[48]M. Piacentini, Solid State Commun. **17**, 697 (1975).
[49]A. Zunger and A. J. Freeman, Phys. Rev. B **16**, 2901 (1977).
[50]N. F. Mott and R. W. Gurney, *Electronic Processes in Ionic Crystals* (Dover, New York, 1964), pp. 80 and 114.
[51]M. R. Pederson and C. C. Lin, J. Chem. Phys. **88**, 1807 (1988).
[52]C. S. Wang and W. E. Pickett, Phys. Rev. Lett. **51**, 597 (1983).
[53]W. E. Pickett and C. S. Wang, Phys. Rev. B **30**, 4719 (1984); Int. J. Quantum Chem. Symp. **20**, 299 (1986).
[54]J. C. Slater, *Quantum Theory of Atomic Structure* (McGraw-Hill, New York, 1960), Vol. II.
[55]J. C. Slater, *Quantum Theory of Molecules and Solids* (McGraw-Hill, New York, 1963), Vol. II.
[56]T. C. Koopmans, Physica **1**, 104 (1933).
[57]A. C. Hurley, *Introduction to Electron Theory of Small Molecules* (Academic, New York, 1976).
[58]M. R. Pederson, Ph.D. thesis, University of Wisconsin, 1986 (unpublished).